Synthesis and Optical Features of ZnO, CuO, and TiO2 Nano-colloids Prepared by Laser Ablation

Adawiya J. Haider[1, a)], Takwa Sadeq Edan[1, b)], Fatima I. Sultan[1, c)], Chafic Salame[2, d)], Lara M. Talib[3, e)] and Murtadha K. Salman[4, f)]

[1] *College of Applied Sciences, University of Technology- Iraq, Baghdad, Iraq.*
[2] *European Academy for Sustainable Development, EURACA, 11, rue du Rempart Saint Thiébault, 57 000, METZ, France.*
[3] *College of Science for Women, University of Baghdad, Baghdad, Iraq.*
[4] *Ministry of Education - Babylon Education Directorate, Babylon Province, Iraq.*

[a)] *Corresponding author: adawiya.j.haider@uotechnology.edu.iq*
[b)] *takwaedan@gmail.com*
[c)] *Fatima.I.Sultan@uotechnology.edu.iq*
[d)] *chafic.salame@euraca.edu.eu*
[e)] *Laramt054@gmail.com*
[f)] *murtadha.phy11@gmail.com*

Abstract. This study presents the synthesis and characterisation of zinc oxide (ZnO), copper oxide (CuO), and titanium dioxide (TiO_2) nanoparticles fabricated through Pulsed Laser Ablation in Liquid (PLAIL). A Q-switched Nd: YAG laser was utilised at wavelengths of 532 nm and 1064 nm for ablating high-purity metallic targets. Different analysis methods, UV–Vis spectroscopy, Tauc plot analysis, Energy-Dispersive X-ray Spectroscopy (EDX), and Transmission Electron Microscopy (TEM) for analysing the generated nanoparticles' structural and optical features. The results confirmed that the laser wavelength affects the nanoparticle properties directly. The optimally synthesised nanoparticles were obtained at 532 nm, which demonstrated stronger optical absorption, wider band gaps, smaller particle sizes, and well-dispersed quasi-spherical morphologies because of the effect of quantum confinement. While the obtained nanoparticles at 1064 nm were larger size with reduced absorption. The uniform distribution of the produced nanoparticles at 532 nm corresponds to increased band gaps of ZnO (3.45 eV) and CuO (1.90 eV), which was confirmed by TEM imaging. Furthermore, the purification and accuracy of the nanoparticles' elemental compositions were further verified by EDX analysis. The current findings highlight the PLAIL potential as a clean and without any additional additives method for customising nanostructures that suit the applications of photocatalytic self-cleaning surfaces and other environmentally sustainable applications.

INTRODUCTION

Various nanomaterials, including metal oxides such as zinc oxide (ZnO), titanium dioxide (TiO_2), and copper oxide (CuO), represent essential materials in modern nanotechnology due to their adjustable optical, structural, and electronic characteristics [1-4]. They are potential and unique candidates for several applications, including photocatalysis, antibacterial coatings, and self-cleaning methods, due to their useful features, such as abundance, chemical stability, and environmental compatibility [5–8]. ZnO is one of the distinguished oxides, characterised by its strong ultraviolet absorption and excellent photostability; TiO_2 displayed high chemical stability and notable strength under harsh conditions, whereas the narrow band gap of CuO facilitates the activation of visible light and photocatalytic activity extending into the solar spectrum. These materials play a role in the activation the depending on the size and morphology, when fabricated at the nanoscale, such as quantum confinement and charge separation improvement, interestingly enhancing their efficiency in light-driven environmental remediation processes [9–12].

The commonly used traditional wet-chemical synthesis techniques are facing challenges, such as contaminating surfactant, toxic reagent additives, and difficulties in controlling the size of the produced particles. Conversely, the Pulsed Laser Ablation (PLAIL) is verified as a green and adjustable top-down procedure with the potential of synthesising nanoparticles with high purity without any stabilising agents or complex precursor requirements. In PLAIL, a high-intensity pulsed laser irradiates a metallic target submerged in a liquid medium, enhancing plasma

formation rapidly, cavitation-bubble dynamics, and nanoparticles formation subsequently. This method allows chemical impurities elemination as well as precisely controlling the particle features via fabricated parameters of the laser, including wavelength, flowability, and duration of the pulse [13-15].

In the current investigation, highly purified metallic Zn, Cu, and Ti targets were ablated in deionised water employing a Q-switched Nd: YAG laser processing at 532 nm and 1064 nm to assess the impact of laser wavelength on the formation of nanostructures. UV–Vis spectroscopy was employed to analyse optical absorption, Tauc analysis was used for the estimation of band-gap energies, and compositional purity was confirmed via Energy-Dispersive X-ray Spectroscopy (EDX). By studying the effects of synthesis parameters on their structural and optical features, this study aims to offer a comprehensive understanding of the generation of wavelength-dependent nanoparticles and explore their applicability in photocatalytic self-cleaning purposes.

EXPERIMENTAL WORKS

Preparation and Formation of ZnO, CuO, TiO2 BY (PLAIL)

Nanoparticles were synthesized using high purity metallic materials, including (Ti), copper (Cu), and zinc (Zn), each possessing a purity level of 99.99%. The Areej Al-Furat Company obtained these targets. Ti and Zn targets were prepared with 0.15 mm thickness, while copper targets had a thickness of 0.10 mm. Pulsed Laser Ablation in Liquid (PLAIL) was employed as the synthesis technique, and the ablation process was carried out in 100 mL of distilled deionized water (DDW) for each sample, which served simultaneously as the dispersion and reaction medium. The resulting nanoparticles were collected and stored in the same deionized water to preserve their structural integrity and prevent agglomeration.

An Nd:YAG laser system (Huafei Tongda Technology – DIAMOND-288 model, EPLS pattern) was used at wavelengths of 532 nm and 1064 nm, with a pulse energy of 1000 mJ and a repetition rate of 10 Hz.

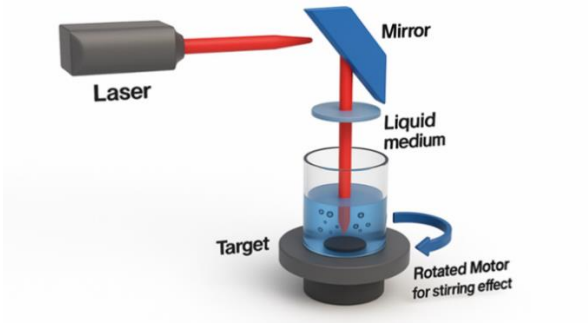

FIGURE 1. Depicts the experimental setup.

TABLE 1 presents the parameters and information about the experiment.

Parameters		Details
Laser Beam	Power	1000mJ
	Number of pulses	Zn (500 pulse), Cu, Ti (600 pulse).
	Wavelength	532nm,1064 nm
	Frequency	10Hz
The Materials	Target	Ti, Cu, Zn plate.
	Liquid	Distilled deionized water (DDW).

Characterization of ZnO, CuO, AND TiO_2 Prepared by Laser Ablation in Liquid

For optical characterization, a Shimadzu UV–Visible double-beam spectrophotometer (model UV-1900, Japan) was employed to investigate the optical absorption spectra of the nanoparticles. Colloidal suspensions were scanned over the wavelength range of 200–700 nanometers to determine their absorption profiles and energy-gap values.

Morphological and compositional analyses were performed using Transmission Electron Microscopy (TEM) and Energy-Dispersive X-ray Scattering (EDX). These techniques were instrumental in describing the structural and elemental properties of the nanostructures they produced.

RESULTS AND DISCUSSION

Absorption UV-Visible Analysis

Pure oxide nanoparticles (ZnO, TiO_2, and CuOH) that have been synthesized through Pulsed Laser Ablation in Liquid (PLAIL) are shown in Figure 2 with their UV-Vis absorption spectra. The effects of two laser wavelengths on the optical properties of the samples were investigated: 532 nm and 1064 nm. Pure oxide absorption reveals that ZnO displays unique electrical transitions at particular energy levels in the UV spectrum (200–350 nm). The shorter wavelength (532 nm) offers more photonic energy, which encourages the creation of nanoparticles with improved optical activity, as can be seen by comparing the photon energies corresponding to the 1064 nm and 532 nm samples [16, 17].

Pure oxides have their strongest absorption, with a broad spectral response from the UV region to around 500 nm. The only exception is TiO_2. A sample formed at 1064 nm is less absorbent than the one made at 532 nm (solid red line) [17].

CuO, despite having a wider spectrum that covers both ultraviolet and visible wavelengths up to 600 nm (in comparison to ZnO and TiO_2, its absorption intensity is lower). Despite the fact that CuO synthesized at 532 nm has slightly greater absorption than that obtained at 1064 nm, it is less noticeable than ZnO and TiO_2..

The overall conclusion is that pure oxides exhibit greater optical absorption when synthesized at the 532 nm laser wavelength.

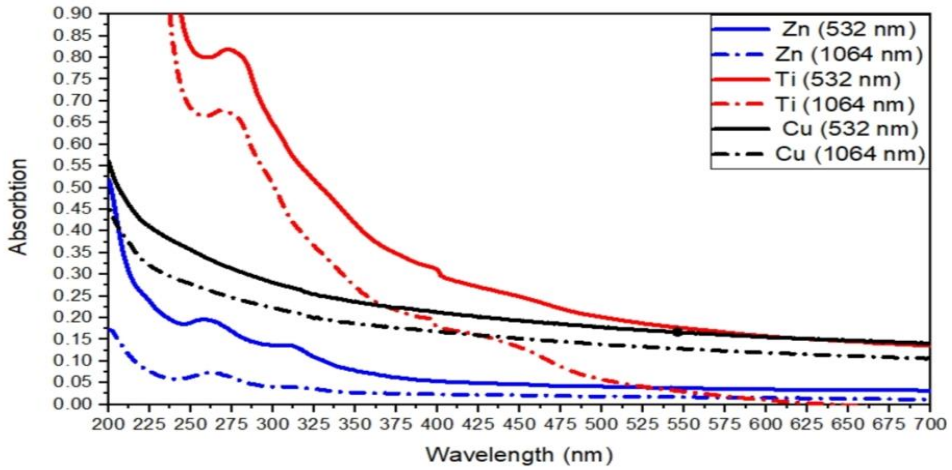

FIGURE 2. Pure oxides (ZnO, TiO_2, CuO) prepared at 532 nm and 1064 nm laser wavelengths are used to obtain UV-Vis absorption spectra for pulsed laser ablated samples in liquid medium.

Energy Band Gap

Figure 3 displays the calculated energy-gap values for samples prepared at laser wavelengths of 532 nm and 1064 nm, respectively. Both particle size and oxide type play a significant role in determining the bandgap values.

When using the 532 nm laser to synthesize pure oxides, the energy gap of ZnO was 3.45 eV times greater than the bulk value of 3.37 eV [19]. The quantum confinement effect, which is caused by the reduction of particle size at this wavelength, is responsible for the increase in blue light, as it increases energy levels and widens the band gap [20]. Studies on ZnO quantum dots with size control indicate that the band gap widens as particle size decreases towards or below the exciton Bohr radius. On the other hand, the ZnO sample produced at 1064 nm had a slightly lower value of 3.35 eV because larger particles are formed to reduce the confinement effect.

At 532 nm, the energy gap of TiO_2 was 3.35 times greater than the bulk value of 3.20 eV [23] than what it was at 1064 nm. At 532 nm, the increase is due to smaller particles and larger surface area, while at 1064, refraction points

to the presence of larger crystallites. Despite the relatively minor difference in band gap between TiO_2 and other materials, it still provides evidence of how much laser wavelength affects nanoscale structural characteristics.

Conversely, CuO underwent a significant transformation from the bulk state (1.40 eV) to the nanoscale. The difference in energy between 532 nm and 1064 nm resulted in a 1.90-eV increase. This widening primarily is caused by strong quantum confinement in CuO nanoparticles, where the band gap increases markedly with reduction of size. The band gap behavior of CuO nanostructures has been demonstrated to be typically between 1.7 and 1.9 eV in previous research [24, 25]. This value is slightly lower than 1064 nm and indicates the formation of particle sizes that are relatively larger.

TABLE 2. Energy gap original elements of ZnO, TiO2, CuO at wavelength 532nm,1064nm.

Material	λ(nm)	E. g(eV) Bulk	E g(eV)	Technical Remarks
ZnO	532	3.25	3.45	Quantum confinement effect (blue shift) due to smaller particle size at 532 nm.
ZnO	1064	3.25	3.35	Larger particle size ⇒ slightly lower Eg compared to 532 nm.
TiO	532	3.20	3.35	Minor Eg variation; enhanced absorption due to higher surface area.
TiO	1064	3.20	3.30	Slight Eg reduction at larger particle sizes.
CuO	532	1.40	1.90	Significant increase in Eg when reduced to nanoscale.
CuO	1064	1.40	1.80	Slightly larger particles at 1064 nm ⇒ lower Eg.

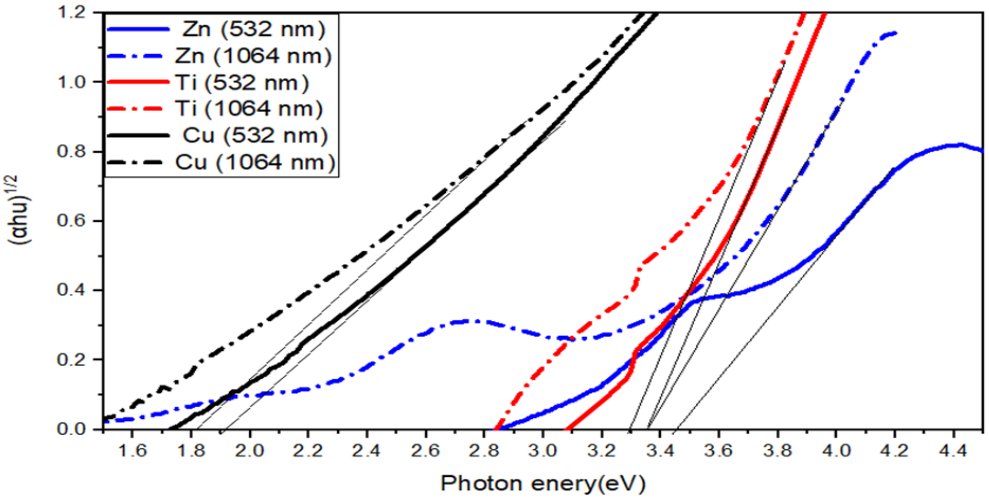

FIGURE 3. Energy gap of pulsed laser ablated samples in liquid medium: pure oxides (ZnO, TiO_2, CuO) prepared at 532 nm, 1064 nm laser wavelengths.

Energy Dispersive X-Ray Spectroscopy (EDX)

For the Zn samples (532 nm and 1064 nm), distinct Zn peaks were observed together with oxygen, verifying the successful formation of ZnO. Note that the Zn peak at exactly 1064 nm was much more intense, sharper, and less faint than that at approximately 532 nm; this is the wavelength-dependent nature of ZNO formation. The dissimilar laser-matter interactions at the two excitation frequencies are a significant contributor to this difference. By increasing the wavelength to 1064 nm, the metallic target is penetrated deeper into the target, and the plasma plume is expanded with a wider range of plasma temperatures. The environment promotes the growth of larger ZnO crystallites with less surface energy due to the aggregation and coalescence of ablated species in this environment. Conversely, with a shorter wavelength (532nm), photon energy is higher at 532 nm and the depth of penetration is lower than that of plasma; this increases ablation rate and makes plasma expansion more explosive. Smaller nuclei condensing into highly dispersed ZnO nanoparticles with finer grain size and narrower size distribution are produced at this wavelength due to the rapid quenching of the plasma plume, which results in a much larger particle.

At 532 nm, the structure of nanoparticles is altered by their faster nucleation and limited coalescence, leading to a higher density of surface-active sites and reduced likelihood of clustering defects. The UV-Vis spectra provide evidence that the nanoscale uniformity is closely linked to enhanced optical transparency and increased excitonic absorption. This is confirmed.In comparison to the bulk ZnO value, the observed larger band-gap value at 532 nm (3.45 eV) suggests that ultrasmall crystallites have a strong quantum confinement effect. With a somewhat higher defect density and a smaller surface-to-volume ratio, ZnO nanoparticles produced with a 1064 nm laser, on the other hand, have the potential to produce localized energy states within the band gap and, as a result, diminish their overall optical activity. The significance of laser wavelength in affecting nucleation processes and establishing the electronic configuration of ZnO nanostructures is underscored by these results. Improved optical absorption and charge-transfer efficiency are the results of the finer morphology and increased purity at 532 nm, which accounts for the greater performance seen at this wavelength. These nanoparticles are therefore ideal for uses such as self-cleaning surfaces, antimicrobial coatings, and photocatalytic degradation. Furthermore, PLAIL-produced ZnO nanoparticles show shorter effective laser wavelengths than expected, according to EDX and TEM investigations, confirming the idea that these materials have adjustable optical and functional characteristics that make them suitable for environmentally friendly technological applications.

TABLE 3. Elemental composition of pure nanostructures determined by EDX analysis .

Sample type	Wavelength (nm)	Elements detected by EDX	Scientific remarks
ZnO (single)	532	Zn, O	Distinct peaks confirming the formation of pure ZnO with uniform and homogeneous nanostructures.
ZnO (single)	1064	Zn, O	Same elemental composition (Zn, O) detected, though the peaks appear weaker as a result of particle agglomeration and increased particle size.
CuO (single)	532	Cu, O	Clear Cu and O peaks observed, confirming high purity of the copper oxide nanostructures.
CuO (single)	1064	Cu, O	Identical elemental composition detected; however, the peak intensity is lower than that observed at 532 nm, indicating reduced purity or increased particle aggregation.
TiO_2 (single)	532	Ti, O	high purity and finer nanoparticle size.
TiO_2 (single)	1064	Ti, O	Same elements, but with less intense peaks due to particle growth.

Transmission Electron Microscopy (TEM) Analysis

Figure 5 (a–c) presents TEM micrographs confirming the successful synthesis of pure ZnO, CuO, and TiO_2 nanoparticles via Pulsed Laser Ablation in Liquid (PLAIL) at a wavelength of 532 nm. The success of the shorter laser wavelength in producing nanoparticles with distinct and desired structural features is demonstrated by the different morphological aspects for each oxide that are highlighted in each image [26, 27]. The ZnO nanoparticles in Figure 5a have a quasi-spherical shape, a homogeneous spatial distribution, and little aggregation. The creation of nanosized ZnO particles is confirmed by the strong correlation between this morphology and the increased optical behavior seen in UV-Vis and Tauc studies, which is indicated by a noticeable blue shift in the absorption edge. It is anticipated that these nanoparticles' strong quantum confinement effect and high surface-to-volume ratio will greatly enhance their photocatalytic performance by improving surface reactivity and charge separation.

TEM images of CuO nanoparticles in Figure 5b show tiny clusters of almost spherical particles with a minor amount of aggregation, all while maintaining nanoscale dimensions. A tighter size dispersion in these results shows that PLAIL at 532 nm achieves better particle size control than traditional chemical production techniques. Particle size reduction and surface-related processes are responsible for the observed morphology, which is consistent with the experimentally measured band-gap widening (1.90 eV). As a result, CuO nanoparticles made under these circumstances have better photocatalytic activity and enhanced electrical characteristics.

FIGURE 4. Laser emission with the presence of pure oxides (ZnO, TiO2, CuO) at laser wavelengths of 532 nm and 1064 nm.

The TEM micrograph of the TiO_2 nanoparticles in Figure 5c shows an uneven shape made up of loosely joined aggregates that create a porous network. TiO_2 nanoparticles have a high surface energy and a strong interphase attraction, which causes them to adapt to one another. Nonetheless, there are nanoscale features, and the shape shown

is in line with proven proof of TiO_2 photocatalytic activity. Even in partial aggregation, TiO_2 nanoparticles have effective light-induced reactivity, which makes them perfect for environmental remediation and self-cleaning coatings [26, 30].

Overall, the TEM results clearly show that producing high-quality nanoparticles in ZnO, CuO, and TiO_2 materials using 532 nm laser ablation is a productive and sustainable method. Both optical (UV-Vis, Tauc) and compositional (EDX) investigations are consistent with the quasi-spherical, extremely small (almost aggregating) particle sizes and morphologies seen in the TEM images. The results of structural, optical, and compositional investigations taken together show that nanoparticles synthesized at 532 nm are more pure, uniform, and functionally effective than those made at 1064 nm.

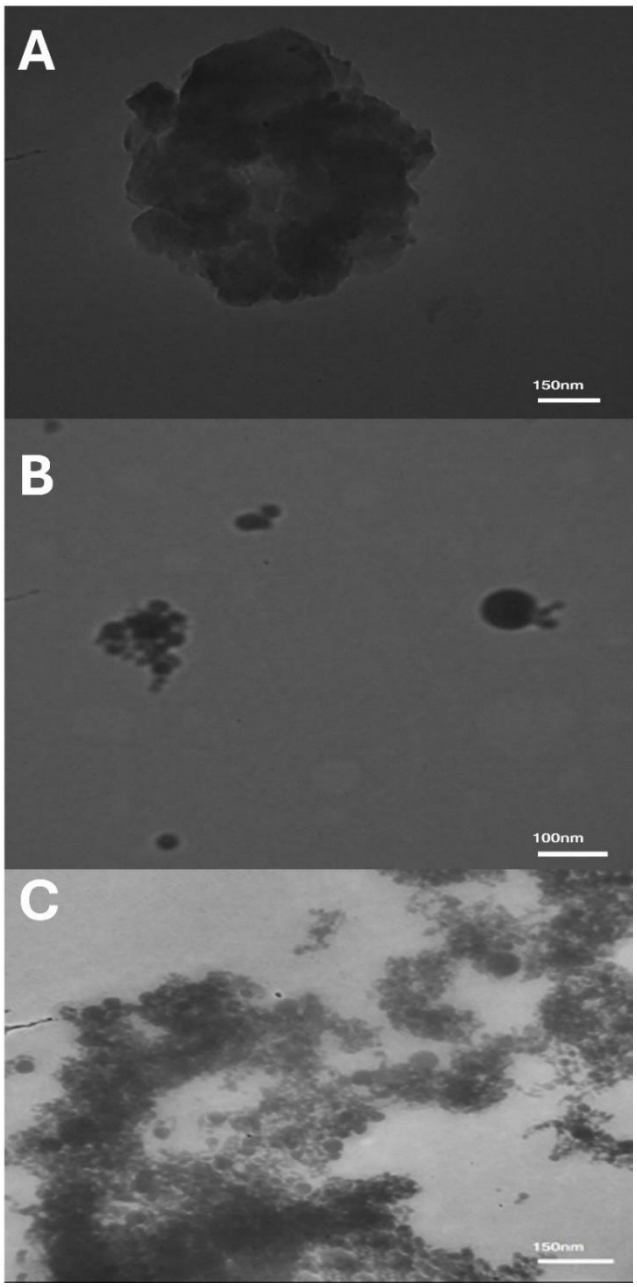

FIGURE 5. TEM picture of pure oxides at 532 nm laser wavelengths: a) ZnO, b) CuO, and c) TiO2 nanoparticles.

CONCLUSION

Because it does not require chemical precursors or surfactants, the synthesis of ZnO, CuO, and TiO_2 nanoparticles using Pulsed Laser Ablation in Liquid (PLAIL) has proven to be an effective and environmentally benign technique. One of the most important variables in regulating the functional and physical attributes of the nanoparticles was found to be the laser wavelength. In contrast to the 1064 nm wavelength, which produced larger particles with relatively lesser optical activity, quantum confinement phenomena at 532 nm encouraged more uniform particle dispersion and improved optical absorption because of higher photon energy.

With stronger elemental peaks for TiO_2 and CuO at 532 nm and better crystallinity for ZnO even at 1064 nm, EDX analysis verified the successful production and high purity of all oxide nanostructures. These results were corroborated by TEM images, which showed that the 532 nm samples included quasi-spherical nanoparticles with little agglomeration. The higher band gaps determined by UV-Vis and Tauc analyses—3.45 eV for ZnO and 1.90 eV for CuO—indicate improved optical characteristics, which are directly correlated with the uniformity and accurate size distribution seen at this wavelength. The chemical purity and nanoscale integrity of the produced materials are further supported by strong elemental signals in the EDX spectra.

All things considered, morphological, structural, and optical data show that 532 nm irradiation creates excellent nanostructures with outstanding antibacterial and photocatalytic capabilities. These findings demonstrate how exact tuning of nanoparticle size, shape, and electronic characteristics is made possible by meticulous control of laser parameters, increasing the functional adaptability of these particles in a range of applications.

REFERENCES

1. J. Haider, A. A. Jabbar, and G. A. Ali, “A review of pure and doped ZnO nanostructure production and its optical properties using pulsed laser deposition technique,” J. Phys. Conf. Ser. 1795, 012015 (2021).
2. Panhwar, S., Buledi, J. A., Mal, D., Solangi, A. R., Balouch, A., & Hyder, A. (2021). Importance and analytical perspective of green synthetic strategies of copper, zinc, and titanium oxide nanoparticles and their applications in pathogens and environmental remediation. *Current Analytical Chemistry*, *17*(8), 1169-1181.
3. Haider, Adawiya J., Maha A. Al-Kinani, and Sharafaldin Al-Musawi. "Preparation and characterization of gold coated super paramagnetic iron nanoparticle using pulsed laser ablation in liquid method." *Key Engineering Materials* 886 (2021): 77-85.
4. Haider, A. J., Sultan, F. I., Haider, M. J., Taha, B. A., Al-Musawi, S., Edan, M. S., ... & Arsad, N. (2024). Characterization of laser dye concentrations in ZnO nanostructures for optimization of random laser emission performance. *International Journal of Modern Physics B*, *38*(08), 2450111.
5. Y. Al-Douri, A. J. Haider, A. H. Reshak, A. Bouhemadou, and M. Ameri, “Structural investigations through cobalt effect on ZnO nanostructures,” Optik 127, 10102–10107 (2016).
6. J. Haider, F. I. Sultan, M. J. Haider, and N. M. Hadi, “Spectroscopic and structural properties of zinc oxide nanosphere as random laser medium,” Appl. Phys. A 125, 2529 (2019).
7. Palivos, Marios, Georgios A. Vokas, Anestis Anastasiadis, Panagiotis Papageorgas, and Chafic Salame. "Comparison study of the technical characteristics and financial analysis of electric battery storage systems for residential grid." In *AIP Conference Proceedings*, vol. 1968, no. 1, p. 030076. AIP Publishing LLC, 2018.
8. Attallah, Ali H., Farah Shamil Abdulwahid, Hayder J. Abdulrahman, Adawiya J. Haider, and Yasir A. Ali. "Investigate toxicity and control size and morphological of iron oxide nanoparticles synthesis by PLAIL method for industrial, environmental, and medical applications: a review." *Plasmonics* 20, no. 3 (2025): 1491-1521.
9. J. Haider, A. D. Thamir, A. A. Najim, and G. A. Ali, “Improving efficiency of TiO_2:Ag/Si solar cell prepared by pulsed laser deposition,” Plasmonics 12, 105–115 (2016).
10. Taha, Bakr Ahmed, Yousif Al Mashhadany, Qussay Al-Jubouri, Adawiya J. Haider, Vishal Chaudhary, Retna Apsari, and Norhana Arsad. "Uncovering the morphological differences between SARS-CoV-2 and SARS-CoV based on transmission electron microscopy images." *Microbes and infection* 25, no. 8 (2023): 105187.
11. S. F. Abbas, A. J. Haider, S. Al-Musawi, and M. K. Selman, “Antibacterial effect of copper oxide nanoparticles prepared by laser production in water against Staphylococcus aureus and Escherichia coli,” Plasmonics (2023).
12. Sidawi, Jihad, Carine Zaraket, Roland Habchi, Nathalie Bassil, Chafic Salame, Michel Aillerie, and Jean-Pierre Charles. "Evolution of photovoltaic solar modules dark properties after exposition to electrical reverse stress current inducing thermal effect." *Microelectronics International* 31, no. 2 (2014): 90-98.
13. S. M. Talib, A. J. Haider, S. Al-Musawi, F. S. Al-Joudi, and S. A. Ahmed, “Laser-fabricated metal oxide core–shell nanoparticles for biomedical applications: A mini review,” Plasmonics (2025).

14. Attallah, Ali H., Farah Shamil Abdulwahid, Yasir A. Ali, and Adawiya J. Haider. "Investigate the Effect of Acidic Environment on the Characteristics and Antibacterial Activity of Al2O3 Nanoparticles Prepared by Laser Ablation." *Lasers in Manufacturing and Materials Processing* (2025): 1-23.
15. Aljbar, N. A., Mahdi, B. R., Khalid, A. H., Attallah, A. H., Abdulwahid, F. S., & Haider, A. J. (2025). Enhanced surface plasmon resonance (SPR) fiber optic sensor for environmental monitoring: a coreless fiber–based design. *Plasmonics*, *20*(2), 605-614.
16. Kadhim, A. M. Haleem, and R. H. Abass, "Anti-dermatophyte activity of TiO_2 NPs colloidal prepared by pulsed laser ablation in liquid environment," Adv. Environ. Biol. 10, 43–54 (2016).
17. Mahdi, Salih Abdul, Afraa Ali Kadhim, Salim Albukhaty, Safoora Nikzad, Adawiya J. Haider, Sumayah Ibraheem, Haitham Ali Kadhim, and Sharafaldin Al-Musawi. "Gene expression and apoptosis response in hepatocellular carcinoma cells induced by biocompatible polymer/magnetic nanoparticles containing 5-fluorouracil." *Electronic Journal of Biotechnology* 52 (2021): 21-29.
18. J. Theerthagiri, et al., "Fundamentals and comprehensive insights on pulsed laser synthesis of advanced materials for diverse photo- and electrocatalytic applications," Light Sci. Appl. 11, 1 (2022).
19. V. N. Jafarova and G. S. Orudzhev, "Structural and electronic properties of ZnO: A first-principles density-functional theory study within LDA(GGA) and LDA(GGA)+U methods," Solid State Commun. 325, 114166 (2021).
20. J. Thyr, J. Montero, L. Österlund, and T. Edvinsson, "Energy alignment of quantum-confined ZnO particles with copper oxides for heterojunctions with improved photocatalytic performance," ACS Nanosci. Au 2, 128–139 (2021).
21. K.-F. Lin, H.-M. Cheng, H.-C. Hsu, L.-J. Lin, and W.-F. Hsieh, "Band gap variation of size-controlled ZnO quantum dots synthesized by sol–gel method," Chem. Phys. Lett. 409, 208–211 (2005).
22. P. K. Samanta, "Band gap engineering, quantum confinement, defect mediated broadband visible photoluminescence and associated quantum states of size tuned zinc oxide nanostructures," Optik 221, 165337 (2020).
23. Wach, et al., "Towards understanding the TiO_2 doping at the surface and bulk," X-Ray Spectrom. 52, 261–268 (2023).
24. M. A. Khan, N. Nayan, S. Shadiullah, M. K. Ahmad, and C. F. Soon, "Surface study of CuO nanopetals by advanced nanocharacterization techniques with enhanced optical and catalytic properties," Nanomaterials 10, 1298 (2020).
25. H. T. Gebrie, et al., "Biosynthesis and characterization of copper oxide nanoparticles from Plumbago zeylanica leaf extract for antibacterial and antioxidant activities," Sci. Rep. 15, 10700 (2025).
26. J. Abdullah, "Optical, structural, and morphological characterization of titanium oxide (TiO_2) nanoparticles from laser ablation in deionized water," J. Wasit Sci. Med. 17, 23–30 (2024).
27. Attallah, Ali H., Farah Shamil Abdulwahid, Yasir A. Ali, and Adawiya J. Haider. "Enhanced characteristics of iron oxide nanoparticles for efficient pollutant degradation via pulsed laser ablation in liquid." *Plasmonics* 19, no. 5 (2024): 2581-2594.
28. M. Al-Asady, A. H. Al-Hamdani, and M. A. Hussein, "Study the optical and morphology properties of zinc oxide nanoparticles," Proc. 2nd Int. Conf. Mater. Eng. Sci. (IConMEAS 2019), AIP Conf. Proc. 2290, 020025 (2020).
29. M. B. Gawande, et al., "Cu and Cu-based nanoparticles: Synthesis and applications in catalysis," Chem. Rev. 116, 3722–3811 (2016).
30. M. M. Rashid, B. Simončič, and B. Tomšič, "Recent advances in TiO_2-functionalized textile surfaces," Surf. Interfaces 22, 100890 (2021).